

caspase-8 became enzymatically active after TCR stimulation (Fig. 3H and fig. S8G). Hence, NF- κ B activation by antigen receptors requires enzyme activity of full-length caspase-8. In the NF- κ B-activating holocomplex, caspase-8 appears to be bound, unprocessed, and only weakly activated, by contrast to caspase-8 in a death-inducing complex (2, 3).

Caspase-8 now emerges both as a pivotal molecule for death-receptor signaling and as a selective signal transducer for NF- κ B during the early genetic response to an antigen. This explains the requirement for caspase activity and caspase-8 for lymphocyte activation and *c-rel* responses after antigen receptor stimuli (4–7, 19). Full-length, unprocessed, but active caspase-8 serves as a crucial link for the CBM and IKK complexes leading to NF- κ B activation not only in lymphoid cell lines, but also in freshly isolated human lymphocytes (Fig. 3, I and J). After antigen receptor stimulation, MALT1-dependent recruitment of the ubiquitin ligase TRAF6 to the CBM complex may enhance regulatory polyubiquitination of IKK γ (20, 21). IKK γ ubiquitination, but not phosphorylation of IKK α,β , occurred in the absence of caspase-8, indicating that ubiquitination may be necessary but not sufficient for IKK activation (fig. S8H).

CED patients manifest certain diagnostic criteria for ALPS, most notably impaired lymphocyte apoptosis (22). However, the combined T, B, and NK cell immunodeficiency is not seen in ALPS patients with Fas, Fas ligand, or caspase-10 mutations. Our findings reveal how a single protease regulates both lymphocyte proliferation and programmed death through different molecular forms. The molecular mechanism we have unveiled may be useful in understanding and treating other varieties of immunodeficiency and disordered lymphocyte homeostasis.

References and Notes

1. A. Ashkenazi, V. M. Dixit, *Science* **281**, 1305 (1998).
2. K. M. Boatright et al., *Mol. Cell. Biol.* **11**, 529 (2003).
3. M. Donepudi, A. Mac Sweeney, C. Briand, M. G. Grutter, *Mol. Cell. Biol.* **11**, 543 (2003).
4. H. J. Chun et al., *Nature* **419**, 395 (2002).
5. L. Salmena et al., *Genes Dev.* **17**, 883 (2003).
6. N. J. Kennedy, T. Kataoka, J. Tschopp, R. C. Budd, *J. Exp. Med.* **190**, 1891 (1999).
7. A. Alam, L. Y. Cohen, S. Aouad, R. P. Sekaly, *J. Exp. Med.* **190**, 1879 (1999).
8. S. Ghosh, M. Karin, *Cell* **109**, S81 (2002).
9. Q. Li, I. M. Verma, *Nat. Rev. Immunol.* **2**, 725 (2002).
10. Materials and methods are available as supporting material on Science Online.
11. B. Zarnegar et al., *Proc. Natl. Acad. Sci. U.S.A.* **101**, 8108 (2004).
12. E. E. Varfolomeev et al., *Immunity* **9**, 267 (1998).
13. Z. Sun et al., *Nature* **404**, 402 (2000).
14. X. Lin, A. O'Mahony, Y. Mu, R. Geleziunas, W. C. Greene, *Mol. Cell. Biol.* **20**, 2933 (2000).

15. M. Thome, *Nat. Rev. Immunol.* **4**, 348 (2004).
16. P. C. Lucas, L. M. McAllister-Lucas, G. Nunez, *J. Cell Sci.* **117**, 31 (2004).
17. P. C. Lucas et al., *J. Biol. Chem.* **276**, 19012 (2001).
18. L. Yu, M. J. Lenardo, *Science* **302**, 1515 (2003).
19. M. Falk et al., *J. Immunol.* **173**, 5077 (2004).
20. L. Sun, L. Deng, C. K. Ea, Z. P. Xia, Z. J. Chen, *Mol. Cell. Biol.* **14**, 289 (2004).
21. H. Zhou et al., *Nature* **427**, 167 (2004).
22. M. C. Sneller et al., *Blood* **89**, 1341 (1997).
23. Molecular interaction data have been deposited in the Biomolecular Interaction Network Database (BIND) with accession codes 196525, 196526, 196446, and 196449. We thank I. Stefanova for tyrosine phosphorylation experiments; V. Barr and L. Samelson for T cell spreading experiments; E. Lee and G. Wang for technical assistance; J. Blenis, R. Siegel, L. Van Parijs, V. Horejsi, A. Jain, V. Dixit, M. Peter, and Z. Liu for materials and reagents; D. Stephany, K. Holmes, and O. Schwartz for flow cytometry and microscopy assistance; F. Dugan and J. Davis for clinical assistance; L. Sun, Z. Chen, Z. Liu, and S. Feske for advice on IKK kinase assay and calcium flux; L. Yu and R. Siegel for helpful discussions; and R. Germain, L. Samelson, and J. Puck for critically reading the manuscript. H.S. is a fellow of the Cancer Research Institute. N.B. is supported by an Association pour la Recherche contre le Cancer (ARC) fellowship.

Supporting Online Material

www.sciencemag.org/cgi/content/full/307/5714/1465/DC1
 Materials and Methods
 SOM Text
 Figs. S1 to S8
 References

1 September 2004; accepted 4 January 2005
 10.1126/science.1104765

Impaired Thermosensation in Mice Lacking TRPV3, a Heat and Camphor Sensor in the Skin

Aziz Moqrich,^{1,2*} Sun Wook Hwang,^{1*} Taryn J. Earley,¹ Matt J. Petrus,² Amber N. Murray,¹ Kathryn S. R. Spencer,¹ Mary Andahazy,² Gina M. Story,¹ Ardem Patapoutian^{1,2†}

Environmental temperature is thought to be directly sensed by neurons through their projections in the skin. A subset of the mammalian transient receptor potential (TRP) family of ion channels has been implicated in this process. These "thermoTRPs" are activated at distinct temperature thresholds and are typically expressed in sensory neurons. TRPV3 is activated by heat (>33°C) and, unlike most thermoTRPs, is expressed in mouse keratinocytes. We found that TRPV3 null mice have strong deficits in responses to innocuous and noxious heat but not in other sensory modalities; hence, TRPV3 has a specific role in thermosensation. The natural compound camphor, which modulates sensations of warmth in humans, proved to be a specific activator of TRPV3. Camphor activated cultured primary keratinocytes but not sensory neurons, and this activity was abolished in TRPV3 null mice. Therefore, heat-activated receptors in keratinocytes are important for mammalian thermosensation.

Thermosensation is thought to be directly mediated by sensory neurons of the dorsal root ganglia (DRGs) that terminate as free nerve endings within the dermal and epidermal layers of the skin (1). Six members of the TRP family of ion channels are activated by distinct thresholds of temperature (2). The expression of most of these thermoTRPs in

DRG neurons is consistent with a role in thermosensation. TRPV3 is activated by warm temperatures above 33°C and exhibits increased response at noxious higher temperatures (3–5). Mouse TRPV3 is distinct among thermoTRPs because it is expressed in keratinocytes but not in DRGs (3). TRPV4, a related innocuous heat-activated ion channel,

is expressed in both DRGs and skin (6–8). The prevailing model that temperature is sensed directly by DRG neurons calls into question whether keratinocyte-derived TRPV3 is involved in thermosensation.

To specifically determine the in vivo function of TRPV3, we used a knockout construct to target the mouse gene encoding TRPV3 by deleting exons encoding the putative pore region and adjacent transmembrane segments five and six, essential domains of the ion channel (fig. S1A). Mice carrying two alleles of the TRPV3 mutation survived through adulthood at the expected Mendelian ratio (fig. S1B). The reverse transcription polymerase chain reaction (RT-PCR) was used to evaluate the expression of TRPV3 in the mutant mice. We used two sets of primers to evaluate TRPV3 transcripts, one pair spanning the deleted region and another preceding it (fig. S1, A and C) (9). TRPV3 transcript from the skin of homozygous knockout mice was not detected with the first pair of primers and was detected at low levels with the second pair (fig. S1C). In contrast,

¹Department of Cell Biology, Scripps Research Institute, La Jolla, CA 92037, USA. ²Genomics Institute, Novartis Research Foundation, San Diego, CA 92121, USA.

*These authors contributed equally to this work.
 †To whom correspondence should be addressed.
 E-mail: ardem@scripps.edu

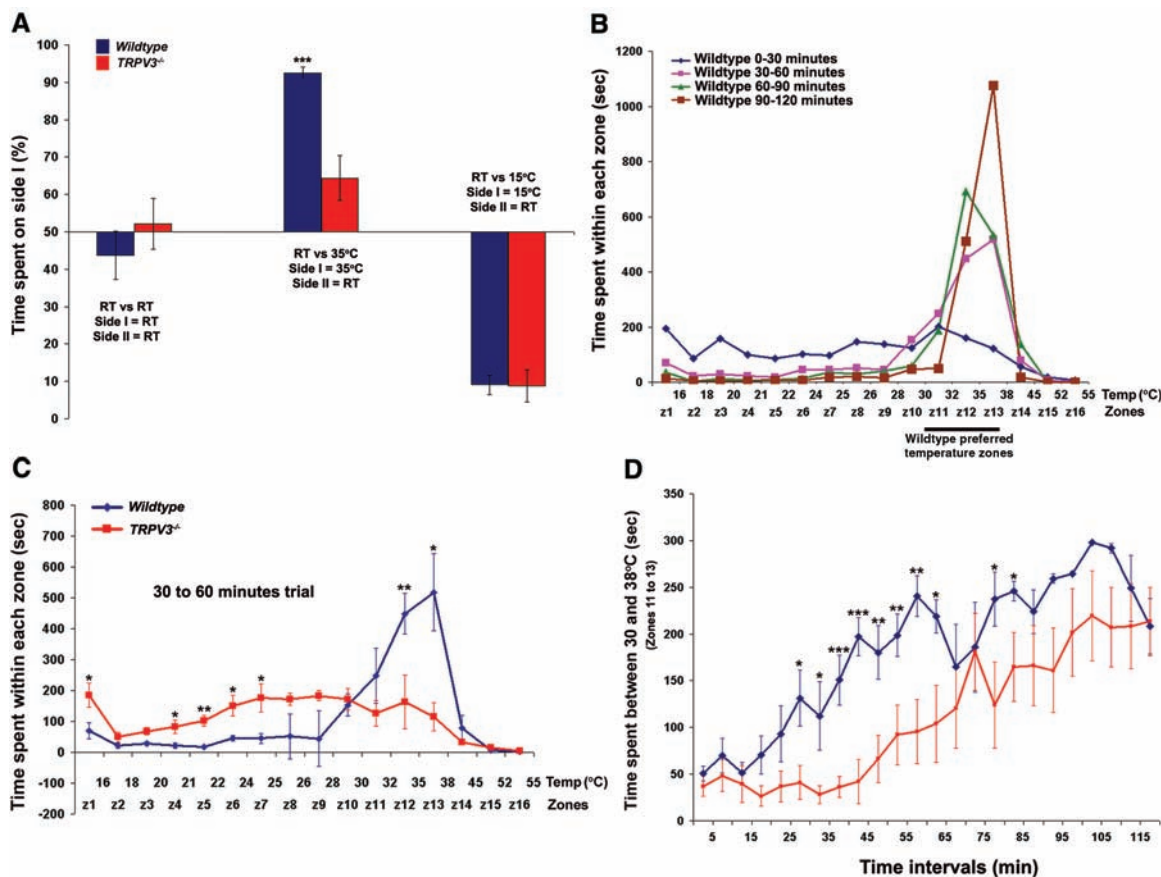


Fig. 1. Mice lacking TRPV3 have a profound deficit in sensing warm temperature in two novel thermotaxis assays. (A) Behavior of wild-type mice and TRPV3^{-/-} littermates on the two-temperature choice test. (B) Behavior of wild-type mice on the gradient assay over a 2-hour trial, shown in 30-min intervals. (C) Behavior of wild-type and TRPV3^{-/-} mice on the gradient from 30 to 60 min. (D) Time spent within the preferred zones (11 to 13) for wild-type and TRPV3^{-/-} mice at each 5-min interval during the 2-hour trial. **P* < 0.05, ***P* < 0.01, ****P* < 0.001.

transcripts of F-actin and TRPV4 were present at normal levels in the knockout mice. Therefore, the deletion resulted in low levels of truncated TRPV3 transcript that does not encode critical pore and transmembrane domains, and there was no detectable compensatory up-regulation of TRPV4 expression in the presence of this mutation.

The mouse gene encoding TRPV3 is 9 kb away from the gene encoding TRPV1, the noxious heat and capsaicin-activated ion channel (3). However, the expression of TRPV1 in DRGs of wild-type and mutant mice appeared indistinguishable, which suggests that TRPV3 deletion results in no major effect on TRPV1 (fig. S1D). Indeed, 25% of neurons were positive for TRPV1 in both wild-type mice (550 of 2226) and TRPV3^{-/-} mice (588 of 2342). We also tested TRPV3^{-/-} mice for their behavioral response to capsaicin and found normal paw licking and/or shaking responses relative to wild-type littermates (fig. S1E). These results show that TRPV1 is expressed normally in TRPV3^{-/-} mice.

We also determined whether the TRPV3 mutation caused anatomical aberrations in DRG projections. Calcitonin gene-related peptide (CGRP) marks DRG neurons that project to the skin. An antibody to CGRP applied to skin sections revealed that this subset of DRG neurons correctly projects to the epidermal-dermal layer in TRPV3^{-/-} mice, corroborat-

ing results obtained with capsaicin injections (fig. S1, D and E). Collectively, the results show that TRPV3^{-/-} mice lack functional TRPV3 without affecting TRPV1 and TRPV4 expression or overall DRG anatomy.

Mice carrying two alleles of the TRPV3 mutation appeared morphologically normal, with normal body weight, internal temperature, and open-field response profiles (fig. S2, A to C). The open-field assay demonstrates that TRPV3^{-/-} mice do not have abnormalities in motor activity or anxiety (10). In some TRPV3^{-/-} mice, a subtle and temporary hair irregularity in the abdominal area occurred around the third postnatal week. Because TRPV3 is expressed in keratinocytes, we investigated whether loss of TRPV3 caused anatomical skin defects. Newborn wild-type mice and their TRPV3^{-/-} littermates excluded toluidine blue dye, which indicated that the epidermal barrier was intact (9, 11). Light and electron microscopic examinations of the epidermis and dermis of TRPV3^{-/-} mice showed no aberrations throughout development and adulthood (fig. S3, A to H) (9). The staining pattern obtained with a panel of keratinocyte markers also appeared normal in TRPV3^{-/-} mice (fig. S3, G and H) (9). We also measured the thickness of the skin and found both the epithelial and dermal layers of TRPV3^{-/-} mice to be similar to their wild-type littermates (fig. S3I). Together these

results show that the anatomy of the skin is normal in TRPV3^{-/-} mice.

Although behavioral tests in rodents for noxious heat are well described, there are few assays for responses to innocuous heat (30° to 42°C). Because TRPV3 is activated by warm temperatures, we established thermotaxis assays to analyze TRPV3^{-/-} mice. In the first test, mice were presented with a choice of occupying a warm surface versus a room-temperature (RT) surface. When both plates were set to RT, wild-type and TRPV3^{-/-} mice spent about 50% of the time on each side (Fig. 1A), a response profile not statistically different from a hypothetical mean of 300 s, or 50%, on side I (one-sample two-tailed *t* test, *P* = 0.35 for wild type, *P* = 0.76 for TRPV3^{-/-}, *n* = 15). We then tested 25 wild-type mice and 29 TRPV3^{-/-} littermates in the 35°C (warm) versus RT preference test (Fig. 1A). Wild-type mice spent on average 92% of the time (554/600 s) on side I, demonstrating a strong behavioral bias toward innocuous warmth. TRPV3^{-/-} littermates spent only 64% of the time (386/600 s) on side I. The difference in response times between wild-type and mutant mice was highly significant (two-sample two-tailed *t* test, *P* = 7.3 × 10⁻⁵). Nonetheless, TRPV3^{-/-} mice still showed a slight bias toward the 35°C side as their response profile statistically deviated from a 300 s (50% on side I) hypothetical mean

(one-sample two-tailed *t* test, *P* = 0.022). This implies that other proteins, most likely TRPV4, are also involved in innocuous thermosensation (8, 12). TRPV3^{+/-} and TRPV1^{-/-} mice behaved like wild-type mice in the 35°C versus RT test; hence, TRPV3 may have a specific role in this thermotaxis behavior (9). When side I of the apparatus was set to a cold temperature of 15°C, both wild-type mice and their TRPV3^{-/-} littermates showed a robust avoidance (92% and 91%, respectively; *n* = 18) of the cooled side, suggesting a crucial role for TRPV3 in heat but not cold sensation.

In another thermotaxis assay, mice were allowed to move freely on a flat rectangular platform (10 cm by 97 cm) with a surface temperature gradient of 15°C to 55°C along the length. The compartment was divided into 16 virtual zones with distinct surface temperature ranges, and the amount of time spent in each zone was recorded. We focused our analysis on four consecutive 30-min intervals (total 2 hours). After some exploration, wild-type mice spent the majority of their time in zones 11 to 13 (temperatures of 30° to 38°C) (Fig. 1C). TRPV3^{-/-} mice showed no significant bias for the preferred zones in the 30- to 60-min interval, a time when wild-type mice had already demonstrated a distinct preference (Fig. 1, B and C). However, after the first hour, the TRPV3^{-/-} mice showed a temperature preference similar to that of wild-type mice (fig. S4, B and C). To highlight the timing of preference, we measured total time spent in the preferred zones (30° to 38°C) during

5-min intervals throughout the 2-hour period (Fig. 1D). Wild-type mice showed strong preference by 25 min, whereas TRPV3^{-/-} mice were severely delayed, not showing preference until 60 min. Together, these experiments confirm an important role for TRPV3 in innocuous thermosensation and suggest that other factors are also involved (8, 12).

TRPV3 is initially activated at warm temperatures (threshold of ~33°C) but also shows an increased response to noxious heat (45° to 48°C) (3). We performed two experiments to test the behavior of TRPV3 null mice in response to moderate and noxious heat temperatures. In the tail immersion assay, the distal part of the tail of a gently restrained mouse was immersed in a thermoregulated water bath, and the time to a reflexive tail flick was recorded. We observed delayed tail flick responses in TRPV3^{-/-} mice at the temperatures tested, with significance achieved at 50°C and above (Fig. 2A). In the hot plate analgesia meter assay, mice were tested for onset of nociceptive behavior (hind paw lick or flick) at three different surface temperatures. Significant withdrawal latencies were observed in TRPV3^{-/-} mice at the higher temperature of 55°C (Fig. 2B). Together, these results show that the response in TRPV3^{-/-} mice to acute noxious heat was disrupted but not abolished. Indeed, the observed acute thermal nociceptive phenotype is similar to those reported for TRPV1^{-/-} mice and suggests that these two TRPV-class ion channels have overlapping function *in vivo* (13, 14).

In addition to an acute thermal phenotype, TRPV1^{-/-} mice also show a strong deficit in thermal hyperalgesia (sensitization

Fig. 2. Mice lacking TRPV3 are deficient in sensing acute noxious thermal stimuli. (A) Onset of nociceptive behavior for wild-type and TRPV3^{-/-} mice in response to tail immersion (*n* = 18). Significant differences are observed at temperatures higher than 48°C. (B) Response latencies to hot plate (for wild type, *n* = 25 for 45°C, *n* = 12 for 50°C, and *n* = 18 for 55°C; for TRPV3^{-/-}, *n* = 29 for 45°C, *n* = 12 for 50°C, and *n* = 18 for 55°C). Significant difference is seen only at the highest temperature tested. **P* < 0.05, ****P* < 0.001.

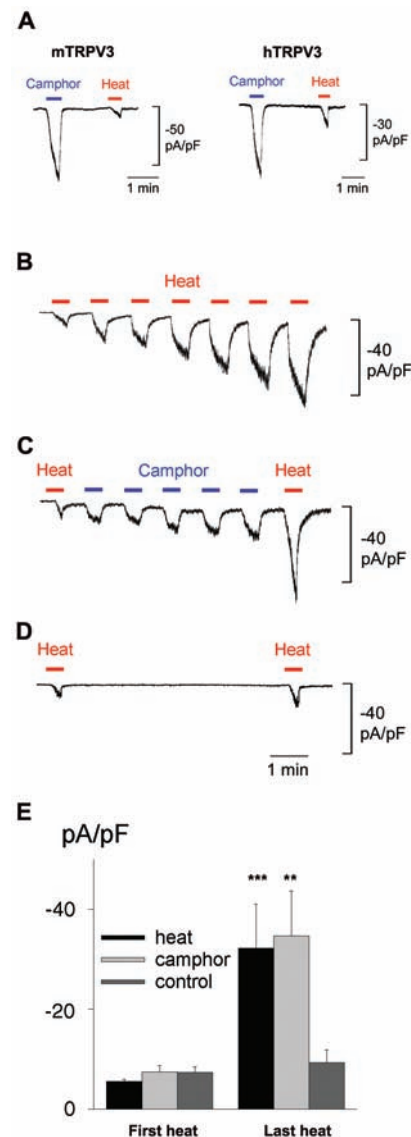
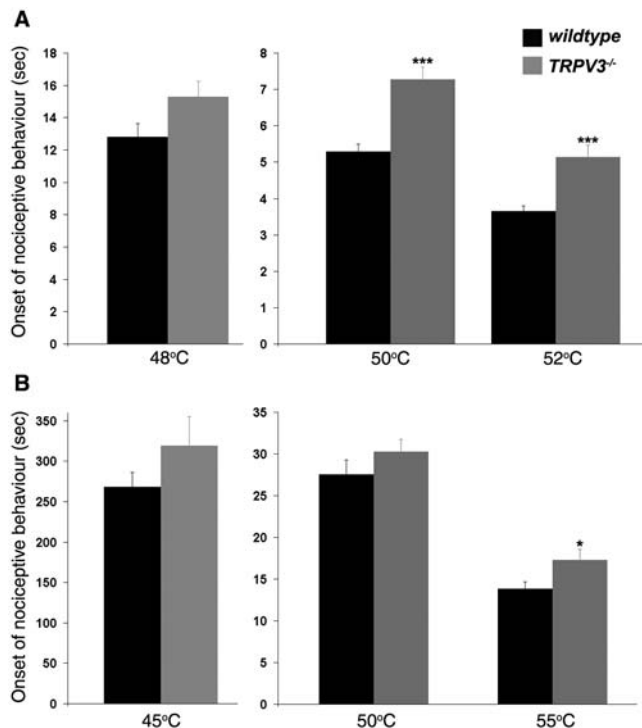


Fig. 3. Camphor activates and sensitizes TRPV3 in CHO cells. (A) Whole-cell currents in mouse and human TRPV3-expressing CHO cells were recorded in response to external application of camphor or a 37°C heat pulse. Camphor (2 mM) elicited large currents from TRPV3-expressing cells (*n* = 6 for mouse TRPV3, *n* = 7 for human TRPV3). (B) Repeated stimulation by heat alone sensitizes the TRPV3 current (*n* = 11). The last heat response was increased by 433 ± 61% (mean ± SE) over the initial heat response. (C) Camphor applications (500 μM) also sensitize TRPV3 responses to heat. The last-to-first heat responses were increased by 433 ± 71% (*n* = 6) [*P*_{camphor} = 0.47 in comparison to heat-induced sensitization in (B)]. (D) In the absence of camphor, a second heat pulse increases the first heat response by only 123 ± 19% (*n* = 8) [*P* = 0.00015 in comparison with (C), two-tailed Student's *t* test]. (E) Average of first and last heat currents from (B), (C), and (D). ***P* < 0.005, ****P* < 0.001.

to noxious thermal stimuli (13, 14). To investigate the role of TRPV3 in hyperalgesia, we injected complete Freund's adjuvant (CFA) or bradykinin into a single hindpaw of wild-type and TRPV3^{-/-} mice. Sensitivity was measured as the response latency to radiant heat stimulation in injected and noninjected hindpaws. Wild-type mice exhibited a significant decrease in the paw withdrawal latencies of the treated paw 24 hours after injection ($n = 12$, one-sample two-tailed t test, $P = 0.00413$ for wild type, $P = 0.028642$ for TRPV3^{-/-}). However, no significant differences were observed in the responses of wild-type and TRPV3^{-/-} mice (fig. S5A). Bradykinin-induced thermal hyperalgesia was also indistinguishable between wild-type and TRPV3^{-/-} mice (fig. S5B). Other nonthermal sensory tests also showed no deficits in TRPV3^{-/-} mice. For example, normal responses to mechanical stimuli (acute or mechanical hyperalgesia) and to injections of formalin (a chemical noxious stimulus) were observed in TRPV3^{-/-} mice (fig. S5, D and E).

Some of the thermoTRPs (TRPV1, TRPM8, and TRPA1) are receptors of sensory compounds that feel hot, cold, or burning (capsaicin, menthol, mustard oil, and cinnamaldehyde), consistent with a physiological

role of these ion channels in thermosensation and pain (2, 15, 16). No sensory compound is known to activate TRPV3. Camphor is a botanical compound used in a variety of topical analgesics and decongestants. Application of camphor on human skin leads to sensitization to heat responses by an unknown mechanism (17). We tested the response of these ion channels to camphor. We found that 1 to 2 mM camphor activated Chinese hamster ovary (CHO) cells expressing human or mouse TRPV3 but not those expressing any of the other five thermoTRPs (Fig. 3A) (9). Activation of TRPV3 by 1 to 2 mM camphor is physiologically relevant, as this chemical is often used in balms at ~10% by weight (corresponding to concentrations of ~0.5 to 1 M).

The effect of camphor on human skin is best characterized as a sensitization to warm temperatures (17). We therefore assessed whether camphor sensitizes TRPV3 responses to warmth. We applied innocuous heat or camphor to TRPV3-expressing cells. Repeated heat pulses of 37°C sensitized TRPV3, as each additional stimulus gave a larger response (Fig. 3, B, D, and E) (3, 5). TRPV3 sensitization to warmth also occurred in response to recurrent activation of the ion channel by camphor (Fig. 3, C and E).

Mouse TRPV3 is specifically expressed in skin keratinocytes (3). We therefore tested whether camphor could also activate and sensitize native TRPV3 in primary cultured keratinocytes. Eighty percent ($n = 56$ of 70) of cultured mouse keratinocytes showed gradually increasing current responses with repeated 37°C pulses. These currents were outwardly rectifying with a reversal potential E_{rev} near 0 mV, similar to the TRPV3 currents when heterologously expressed in CHO cells (Fig. 4A). The majority of cells (66%) were also sensitive to 2 to 10 mM camphor, and the responses to warm temperature (37°C) were robustly potentiated by treatment with camphor (Fig. 4B). Furthermore, 5 μ M ruthenium red (a blocker of TRPV ion channels) completely blocked the camphor-induced currents at negative voltages (fig. S6A). Collectively, these recordings provide strong evidence that camphor activates and sensitizes native TRPV3 expressed in keratinocytes. In our experiments, TRPV3- and TRPV4-like responses are both readily observed in keratinocyte cultures (80% TRPV3-like and 30% TRPV4-like, with a 20% overlap). These data vary from a report that describes TRPV4-like heat responses but few TRPV3-like responses in a majority of keratinocytes (8). However, Chung *et al.*

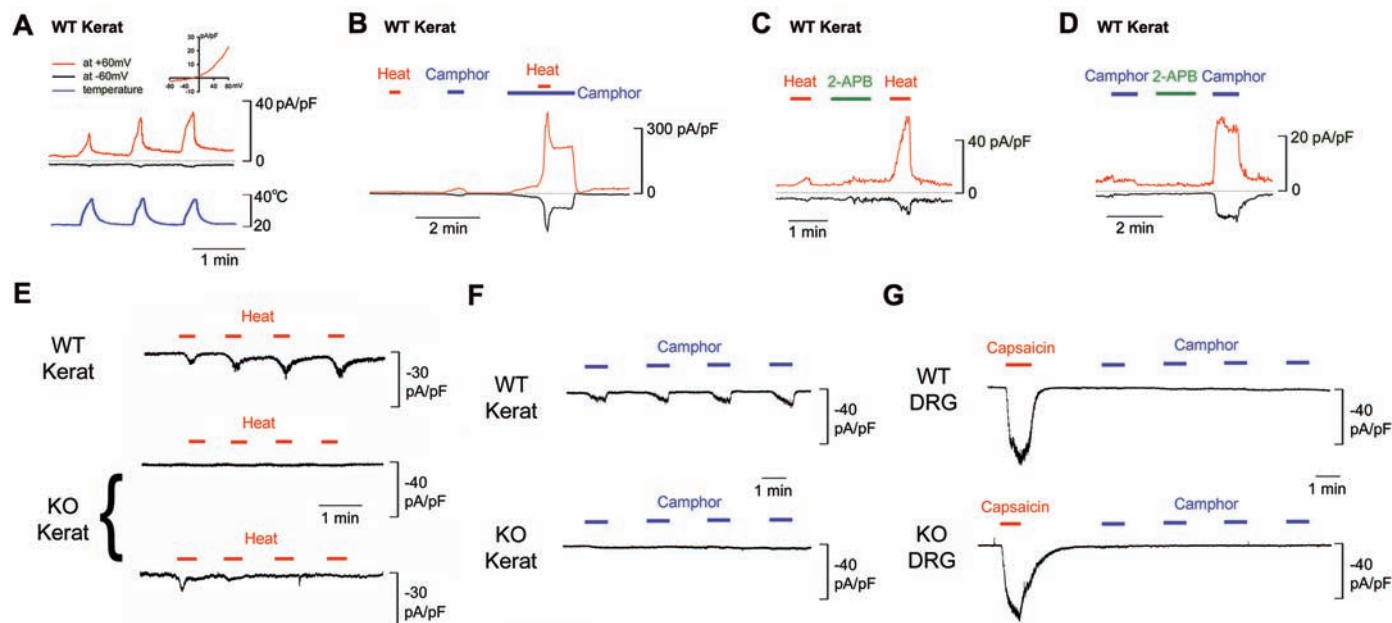


Fig. 4. Heat- and camphor-activated currents in wild-type and TRPV3^{-/-} mice. (A to D) Camphor activates and sensitizes TRPV3 in cultured wild-type keratinocytes. (A) Repeated stimulation of heat gives rise to a TRPV3-like sensitizing current. Inset: Current response upon heat stimulation shows outwardly rectifying current-voltage relationship with E_{rev} near 0 mV. Dotted line, zero current level. (B) Camphor (5 mM) activates an outwardly rectifying current. The heat response of the same cell is greatly increased during application of 5 mM camphor ($n = 10$ of 16 tests, $569 \pm 129\%$, $P = 0.002$). Application of 100 μ M 2-APB sensitizes the response to heat ($n = 5$, $911 \pm 331\%$, $P = 0.0001$) (C) and the response to 2 mM camphor ($n = 5$, $877 \pm 181\%$, $P = 0.003$) (D), respectively. (E) Repeated stimulation by heat activates and sensitizes a TRPV3-like current in keratinocytes from wild-

type littermates (upper trace, recorded at -60 mV, $n = 22$). Other cells show TRPV4-like response ($n = 2$), mixed response ($n = 4$), or no response ($n = 1$) (9). No response (middle trace, $n = 16$) or TRPV4-like rapidly desensitized current (bottom trace, $n = 9$) is observed in TRPV3^{-/-} keratinocytes. TRPV3-like, TRPV4-like, or mixed currents were determined as described (8, 19). (F) Keratinocytes from TRPV3^{-/-} mice do not respond to 5 mM camphor ($n = 34$, bottom trace), whereas those from wild-type littermates show the normal camphor response ($n = 7$ of 9, upper trace). (G) Cultured DRG neurons from wild-type littermates or from TRPV3^{-/-} mice do not respond to repeated application of 5 mM camphor ($n = 43$ and $n = 14$, respectively); 58% of wild-type mouse DRG neurons tested and 57% of those from TRPV3^{-/-} mice show response to 0.5 μ M capsaicin.

observed TRPV3 protein expression in a majority of keratinocytes and detected abundant TRPV3-like responses in the presence of 2-aminoethoxydiphenyl borate (2-APB), a compound that activates and sensitizes TRPV3 (8, 18, 19). Consistent with these reports, we observed that pretreatment with 100 μ M 2-APB strongly potentiated heat and camphor responses in keratinocytes (Fig. 4, C and D), whereas camphor was not capable of sensitizing 2-APB responses ($n = 3$) (9). Together, these studies imply that TRPV3 is present in a majority of cultured keratinocytes.

We next compared the camphor- and heat-induced currents of wild-type and TRPV3^{-/-} littermate keratinocytes. The majority of wild-type keratinocytes showed gradually increasing current responses with repeated 37°C pulses at -60 mV, whereas TRPV3^{-/-} keratinocytes showed no responses or some responses with TRPV4-like desensitization (Fig. 4E) (fig. S6B). Responses to repeated application of 5 mM camphor were observed in wild-type but not TRPV3^{-/-} keratinocytes (Fig. 4F). This suggests that TRPV3 is a heat receptor in keratinocytes, that it is the only receptor for camphor in these cells, and that camphor sensitivity is a specific functional marker for TRPV3. Unlike what was observed for keratinocytes, 5 mM camphor failed to evoke sensitizing current responses from capsaicin-sensitive or capsaicin-insensitive DRG neurons from either wild-type mice ($n = 43$) or TRPV3^{-/-} mice ($n = 14$) (Fig. 4G).

The residual sensitivity to warm temperatures in TRPV3^{-/-} mice may be due to partial compensation by TRPV4, the only other ion channel known to respond to innocuous heat in culture (20, 21). Consistent with expression analysis, camphor activity was observed in keratinocytes but not in DRG neurons, even with high concentrations of camphor. Therefore, the acute thermosensory phenotype observed in TRPV3^{-/-} mice suggests an important role of skin in temperature sensation. Keratinocytes are not known to "sense" temperature; instead, DRGs are thought to directly sense heat through free nerve endings (1). This conclusion is mainly based on the ability of dissected neurons to respond to temperature shifts and on the anatomical observation that no synapses are apparent between free nerve endings and keratinocytes (22, 23). However, a recent study has observed a population of chemosensory cells that form synaptic contacts with trigeminal afferent nerve fibers within the nasal epithelium (24). Furthermore, nonsynaptic communication between keratinocytes and nerve fibers can be considered.

References and Notes

1. H. Hensel, *Monogr. Physiol. Soc.* **38**, 1 (1981).
 2. A. Patapoutian, A. P. Peier, G. M. Story, V. Viswanath, *Nature Rev. Neurosci.* **4**, 529 (2003).

3. A. M. Peier *et al.*, *Science* **296**, 2046 (2002).
 4. G. D. Smith *et al.*, *Nature* **418**, 186 (2002).
 5. H. Xu *et al.*, *Nature* **418**, 181 (2002).
 6. W. Liedtke *et al.*, *Cell* **103**, 525 (2000).
 7. M. Suzuki *et al.*, *Neurosci. Lett.* **353**, 189 (2003).
 8. M. K. Chung, H. Lee, A. Mizuno, M. Suzuki, M. J. Caterina, *J. Biol. Chem.* **279**, 21569 (2004).
 9. A. Moqrich *et al.*, data not shown.
 10. T. Miyakawa, M. Yamada, A. Duttaroy, J. Wess, *J. Neurosci.* **21**, 5239 (2001).
 11. J. Reichelt, H. Büssow, C. Grund, T. M. Magin, *Mol. Biol. Cell* **12**, 1557 (2001).
 12. H. Todaka, J. Taniguchi, J.-i. Satoh, A. Mizuno, M. Suzuki, *J. Biol. Chem.* **279**, 35133 (2004).
 13. J. B. Davis *et al.*, *Nature* **405**, 183 (2000).
 14. M. J. Caterina *et al.*, *Science* **288**, 306 (2000).
 15. S. E. Jordt *et al.*, *Nature* **427**, 260 (2004).
 16. M. Bandell *et al.*, *Neuron* **41**, 849 (2004).
 17. B. G. Green, *J. Invest. Dermatol.* **94**, 662 (1990).
 18. H. Z. Hu *et al.*, *J. Biol. Chem.* **279**, 35741 (2004).
 19. M. K. Chung, H. Lee, A. Mizuno, M. Suzuki, M. J. Caterina, *J. Neurosci.* **24**, 5177 (2004).
 20. A. D. Guler *et al.*, *J. Neurosci.* **22**, 6408 (2002).
 21. H. Watanabe *et al.*, *J. Biol. Chem.* **277**, 13569 (2002).
 22. N. Cauna, *J. Anat.* **115**, 277 (1973).

23. M. Hilliges, L. Wang, O. Johansson, *J. Invest. Dermatol.* **104**, 134 (1995).
 24. T. E. Finger *et al.*, *Proc. Natl. Acad. Sci. U.S.A.* **100**, 8981 (2003).
 25. We thank M. Bandell, B. Conti, H. Esendencia, P. Garrity, S. Kupriyanov, M. Mayford, A. Peier, L. Reijmers, M. Wood, and J. Watson for input and assistance; M. Caterina for sharing a detailed protocol on primary culture of keratinocytes; T. Bartfai for sharing the thermal gradient platform; and N. Hong, T. Jegla, U. Mueller, and L. Stowers for critical reading of the manuscript. Supported by National Institute of Neurological Disorders and Stroke grants R01NS046303 and R01NS42822. G.M.S. is a recipient of a National Research Service Award postdoctoral fellowship from NIH. A.P. is a Damon Runyon Scholar.

Supporting Online Material

www.sciencemag.org/cgi/content/full/307/5714/1468/DC1

Materials and Methods

Figs. S1 to S6

References

13 December 2004; accepted 4 January 2005
 10.1126/science.1108609

OSBP Is a Cholesterol-Regulated Scaffolding Protein in Control of ERK1/2 Activation

Ping-yuan Wang, Jian Weng, Richard G. W. Anderson*

Oxysterol-binding protein (OSBP) is the founding member of a family of sterol-binding proteins implicated in vesicle transport, lipid metabolism, and signal transduction. Here, OSBP was found to function as a cholesterol-binding scaffolding protein coordinating the activity of two phosphatases to control the extracellular signal-regulated kinase (ERK) signaling pathway. Cytosolic OSBP formed a ~440-kilodalton oligomer with a member of the PTPPBS family of tyrosine phosphatases, the serine/threonine phosphatase PP2A, and cholesterol. This oligomer had dual specific phosphatase activity for phosphorylated ERK (pERK). When cell cholesterol was lowered, the oligomer disassembled and the level of pERK rose. The oligomer also disassembled when exposed to oxysterols. Increasing the amount of OSBP oligomer rendered cells resistant to the effects of cholesterol depletion and decreased the basal level of pERK. Thus, cholesterol functions through its interaction with OSBP outside of membranes to regulate the assembly of an oligomeric phosphatase that controls a key signaling pathway in the cell.

Depletion of membrane cholesterol markedly increases the level of pERK in the caveolae and cytosol fractions of cells (1). The level of pERK is increased further by simultaneously exposing the cells to epidermal growth factor (EGF), which suggests that cholesterol depletion inactivates a pERK phosphatase. Recently, we identified a cholesterol-regulated phosphatase that has dual specific activity for pERK (2). When cellular cholesterol levels are normal, this phosphatase works in tandem with the ERK kinase MEK-1 to

regulate the level of pERK in the cell. The phosphatase is a heterooligomer of ~440 kD that derives its dual specific activity from two phosphatases. One is a member of the PTPPBS family of tyrosine phosphatases (3), and the other is the serine/threonine phosphatase PP2A (2). These two enzymes each depend on the activity of the other to coordinately remove phosphate from both the threonine and the tyrosine residues of pERK. Depletion of cell cholesterol results in the dissociation of PP2A from the PTPPBS member and a loss of dual specific pERK phosphatase activity. Thus, cholesterol appears to act directly or indirectly to control the formation of an oligomer of two phosphatases that together have functionality that neither has alone. Here, we present

Department of Cell Biology, University of Texas Southwestern Medical Center, Dallas, TX 75390-9039, USA.

*To whom correspondence should be addressed.
 E-mail: richard.anderson@utsouthwestern.edu